M. C. Miller[a)]
School of Health Sciences,
Duquesne University,
Pittsburgh, Pennsylvania 15212 USA;
Department of Mechanical Engineering,
University of Pittsburgh,
Pittsburgh, Pennsylvania 15621 USA;
Department of Orthopaedic Surgery,
Allegheny General Hospital,
Pittsburgh, Pennsylvania 15212 USA

P. Smolinski
Department of Mechanical Engineering,
University of Pittsburgh,
Pittsburgh, Pennsylvania 15621 USA

S. Conti

K. Galik

Department of Orthopaedic Surgery,
Allegheny General Hospital,
Pittsburgh, Pennsylvania 15212 USA

Stresses in Polyethylene Liners in a Semiconstrained Ankle Prosthesis

A finite element model of a semiconstrained ankle implant with the tibia and fibula was constructed so that the stresses in the polyethylene liner could be computed. Two different widths of talar components were studied and proximal boundary conditions were computed from an inverse process providing a load of five times body weight appropriately distributed across the osseous structures. von Mises stresses indicated small regions of localized yielding and contact stresses that were similar to those in acetabular cup liners. A wider talar component with 36% more surface area reduced contact stress and von Mises stresses at the center of the polyethylene component by 17%.
[DOI: 10.1115/1.1798011]

Introduction

Long term survival of joint replacements is frequently governed by the durability of polyethylene components. Recent developments in implant design and surgical technique have revived the viability of ankle replacement [1–5] by reducing the number of complications due to infection, loosening, and subsidence. With longer-term success, however, problems due to polyethylene wear could arise even if advanced cross-linked polyethylene were used.

Clinical evidence [6–9] has demonstrated the vital problems related to polyethylene wear in hip and knee implants. Wear can lead to osteolysis, polyethylene component failure, and loosening, all of which can necessitate revision surgery. The wear of materials is a function of the contact stresses between articulating surfaces and finite element modeling has successfully analyzed these stresses in hip and knee replacements [10,11]. Computer analysis has thus provided a means to evaluate the effect of design changes without clinical trials.

Stress analysis of polyethylene liners is critical to implant design because the polyethylene is the most likely component to wear or fail. Commonly used ankle replacement systems employ concentric or nearly concentric cylindrical articulating surfaces [12] and the AGILITY system (Depuy, Inc., Warsaw, IN) is representative of this type. This system consists of a tibial tray supporting a polyethylene insert with a concave cylindrical distal surface. The cobalt-chrome talar component is trapezoidally shaped to mimic the anatomic talar morphology and has a cylindrical contact surface with a radius of curvature of 0.076 mm less than the polyethylene concavity. Both the proximal tibial surface and the distal talar surface have porous coatings for bone ingrowth. Surgical procedure includes fusion of the distal tibio-fibular syndesmosis joint.

Design goals for the implant system include low stresses, the ability to translate medio-laterally along the parallel cylindrical axes of the contacting surfaces, and a large interface area on the talus with the talar component. These goals are conflicting be-

cause increasing the width to minimize contact stress and maximize talar interface area decreases the available travel distance.

A few researchers have used computational methods to investigate general aspects of ankle replacement [13–17] but no one has combined design variations within a full, three-dimensional tibio-fibular construct. Furthermore, although previous analyses of polyethylene in total ankles exist [17,18], no work has addressed the effect of talar component width even though a wider component will reduce stresses. Although the edge radius of the component has an effect on stresses, changing this parameter also changes the contact area. A small edge radius provides greater contact area but will increase the stress concentration and a large edge radius will decrease the contact area but also decrease the stress concentration. A large edge radius will also reduce the stability to inversion-eversion moments. Increasing the width of the component without increasing the edge radius is the simplest design change that does not need to consider the effect on inversion-eversion stability. Moreover, a modest increase in width maintains the kinematic feature of medio-lateral translation. Therefore, the hypothesis of this study was that a wider talar component that maintains the primary kinematic conditions of the construct will proportionally reduce stresses.

Methods

A human cadaveric specimen was digitized to develop the geometry for a finite element model. The distal portion of the right lower leg from a 69-year old female was embedded in polymer resin and sectioned in the transverse plane. The tibia, fibula, and talus were embedded together with ligamentous constraints, maintaining their physiologic orientation. A total of 27 sections were taken separated by 1 mm at the tibio-talar joint and by 5 mm in the diaphyseal shaft. The thickness of each slice was recorded and included the saw blade thickness. Each section was optically scanned and endosteal and periosteal boundaries were identified. The interface between the cortical and cancellous bone was marked with 15 equally spaced points and the points were imported into a finite element program (Ansys, Inc., VERSION 5.7, Southpointe, PA). Sequential cubic splines were fitted to the

Copyright © 2004 by ASME

Fig. 1   Solid model of the lower leg

Table 1   Material properties

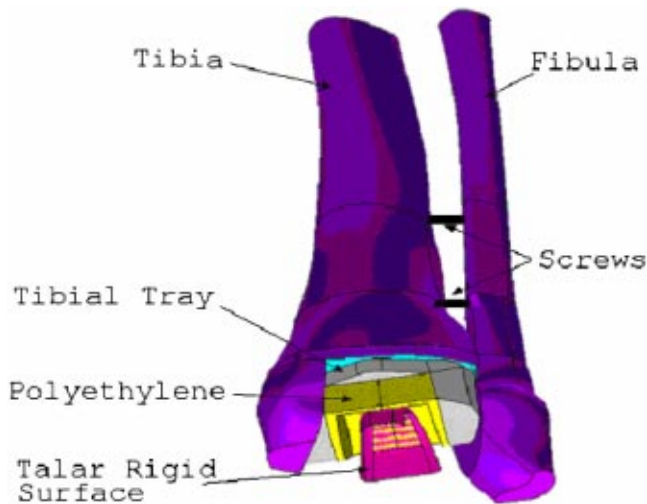| Material	Young's modulus (MPa)	Poisson's ratio
Cortical bone	17,580	0.30
Cancellous bone	280	0.30
Titanium	110,000	0.33
Stainless steel	189,600	0.30

points and the cross-sections outlined by the splines were joined by areas with four sides composed of B-splines. This process recreated the original geometry of bones. (Fig. 1)

To study the effect of talar component width, the stresses resulting from two kinematically satisfactory designs of talar component were analyzed. First, the original trapezoidal shaped was studied and, then, second, a wider design with an increased contact area. (Fig. 2) The trapezoidal shapes permitted more lateral-medial translation with plantar flexion. The wider design maintained most of the original lateral-medial translation because the anterior width was unchanged and still permitted slightly more lateral-medial translation with plantar flexion due to a trapezoidal shape. The wider design increased the inferior talar interface area substantially, which could mean reduced stresses in the talus itself. Stresses in the talus, however, were not a focus of the current study.

The metallic components and bone were discretized using ten node tetrahedral elements, but the layer of cortical bone in the distal tibia and fibula was modeled using four-node quadrilateral shell elements with a thickness of 1.0 mm. The polyethylene mesh consisted of eight-node hexahedral elements. The talus was not needed as will be subsequently discussed. The cortical bone at the syndesmosis fusion was removed, as indicated by the surgical procedure, and the bones were assumed to be perfectly bonded. No soft tissues in the joint or between the bones were modeled. Two stainless steel bone screws with a diameter of 3.5 mm as
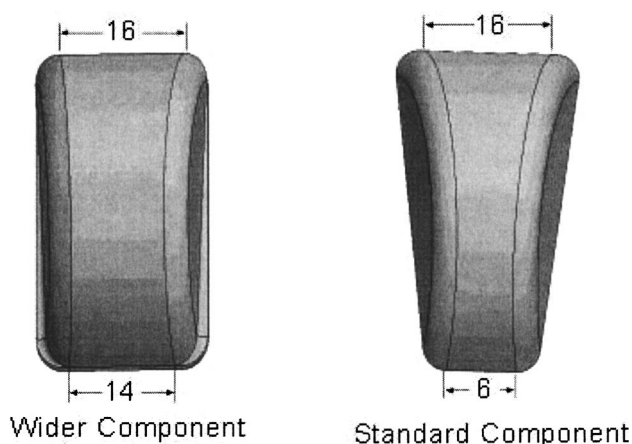
required by the fusion were represented using beam elements with a round cross-section. To simplify the meshing in the vicinity of the screws, the bone in the location of the screws was not removed and the nodes of the beam elements were identical to the nodes of the bone. The implant in the model was positioned under the direction of an experienced surgeon and requisite amount of bone removed. Contact elements were placed between the polyethylene and the talar component, which was modeled as a rigid surface. All other material interfaces were bonded. Even though backside wear has been found to occur in the hip [19], the assumptions of this model did not include contact elements at polyethylene-tibial component interface. The model consisted of 41,597 elements and 68,553 nodes and required 36 hours processing time with an 833 MHz Pentium III computer.

Linear, isotropic, and elastic material properties were used for the bone and implant components [20] except for the polyethylene [21] which had nonlinear properties. The linear material properties are listed in Table 1. The polyethylene true stress-true strain relationship had an initial yield stress of 11 MPa and eight regions of decreasing tangent moduli in the plastic zone as shown in Table 2. A Poisson's ratio of 0.46 was used.

Determination of the proximal load distribution on the tibia and fibula was necessary for this study in order to create appropriate boundary conditions. The proximal traction boundary conditions were computed using an inverse process. It was assumed that the total load carried by the tibia and fibula was five times body weight [22] (body weight=666 N) which is the maximum force applied to the joint during normal gait. In the first step of this process a simulated contact pressure was applied to the bottom of the polyethylene component. The pressure distribution assumed the shape of a haversine in the anterior-posterior direction applied over the projected area of the talar component and was constant in the medial-lateral direction. The loaded area was centered on the polyethylene insert and the amplitude was chosen so that the total force generated by the pressure was 3330 N. It should be noted that due to the wedge shape of the talar component in the anterior-posterior direction, this distribution was not symmetric about the coronal plane. The tibia and fibula were constrained superiorly in the vertical direction and vertical normal traction distribution was determined. It was found that the fibula carried 7% of the load. In the second step of the process in which the polyethylene stresses were computed, the talar component was included and the previously calculated traction distribution was applied in the opposite direction to the proximal ends of the tibia and fibula. The talar component was constrained in all directions and the proximal end of the tibia-fibula model was constrained in the superior-inferior direction and all nodes were constrained in the transverse plane.

Fig. 2   Talar components used in this study

Table 2   Polyethylene stress-strain modeling

True strain	True stress (MPa)
0.0195	10.86
0.0377	15.95
0.0494	18.40
0.0663	20.65
0.0897	22.70
0.1216	24.44
0.2853	31.12
0.3477	33.12

The convergence of the finite element model was assessed by refining the polyethylene component mesh. In the first refinement, the element side length was changed from 0.5 to 0.25 mm which reduced the peak stresses by 10%. In the subsequent refinement, the polyethylene element size was changed to 0.10 mm, which resulted in a change of stresses of 1% in the elements along the apex of the polyethylene concavity. The peak stresses varied less than 3% with the final refinement so that the 0.10 mm size was deemed adequate for the polyethylene. Given that convergence occurs asymptotically, the error in the second refinement must be less than the 10% of the first refinement. The bound of 10% on the second discretization coupled with the 3% change due to the polyethylene mesh refinement indicated that the maximum overestimate of stress due to a 0.25 talar component element size would be 7% (i.e., 10%–3%). The 0.25 mm discretization of the talar edge radius was considered acceptable.

The effect of dorsi-plantar flexion angle on polyethylene stresses was investigated by varying the angle between the proximal tibial and distal talar surfaces. The dorsi-plantar flexion angle was varied from 20 Deg plantar flexion to 20 Deg dorsiflexion in ten degree increments. The same proximal traction boundary conditions were used in all cases.

Results

The edges of the region of contact between the talar and the polythyene components are indicated by elevated von Mises stresses as shown in depiction of the distal surface of the polyethylene (Fig. 3). The peak contact pressures and von Mises stresses for the two implant designs occurred along the talar component edges as shown in Figs. 4 and 5. Note that these two figures show stresses along a path along the frontal midline of Fig. 3 and that the values plotted in Fig. 5 are the maxima, which occur 0.2 mm beneath the surface. Figure 6 clearly illustrates that the peak von Mises stresses occurred beneath the surface. Figure 7 shows that the von Mises stresses through the thickness of the polyethylene at the center of the contact area were at a maximum on the surface, decreasing monotonically with depth. The von Mises stresses, however, at the edges of the contact area increased immediately beneath the surface and remained above 10 MPa through the thickness. The results in Figs. 3–7 are for the neutral tibio-talar orientation.

When considering the effect of plantar and dorsiflexion, all stresses decreased with dorsiflexion by approximately the same percentage for the standard width implant, 18%, from 20 Deg
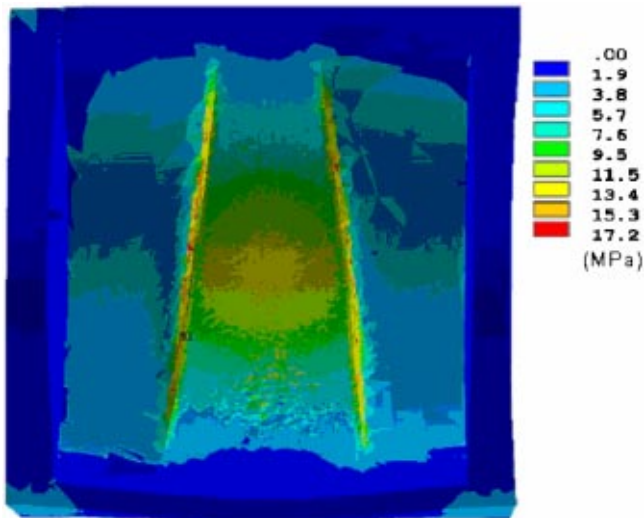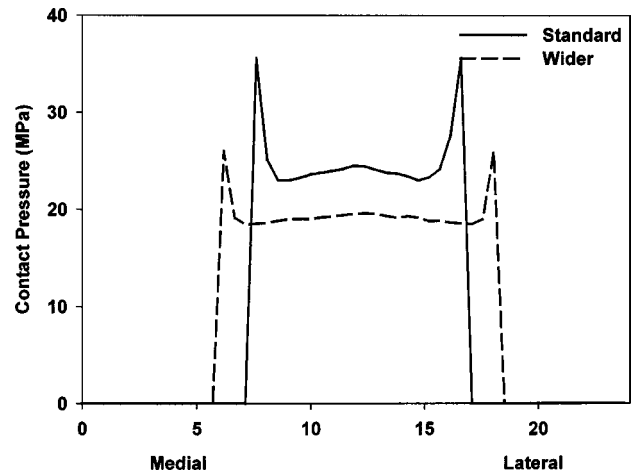

Fig. 4 Contact pressure along the frontal plane at the midline for both talar component designs. The talar component is centrally located relative to the 24 mm wide tibial component.

plantarflexion to 20 Deg dorsiflexion as indicated by Fig. 8. For the wider component, analyses were completed only for the +20, neutral and −20 Deg flexion cases because the changes were small. The stresses for the wider model were smaller in magnitude and had a smaller reduction with dorsiflexion (10%).
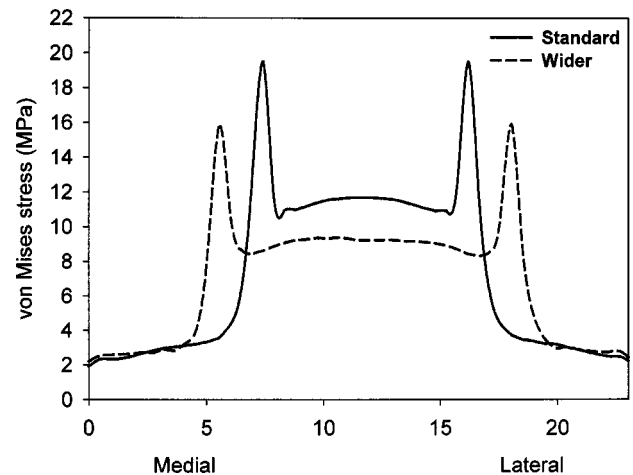

Fig. 5   von Mises stress 0.2 mm beneath the surface along the frontal plane at the midline for both talar component designs. The talar component is centrally located relative to the 24 mm wide tibial component.
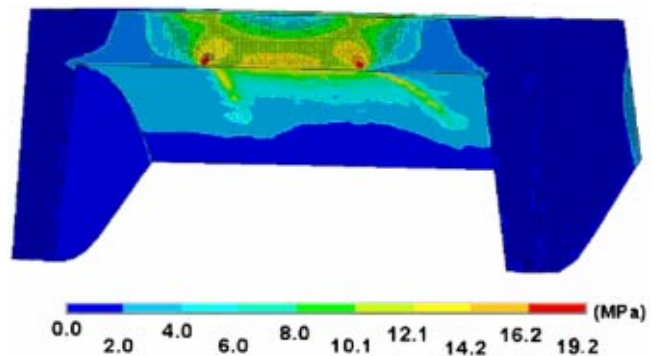

Fig. 6   von Mises stress through the thickness (Standard width implant). Shown is an oblique view of the posterior half of the polyethylene insert.
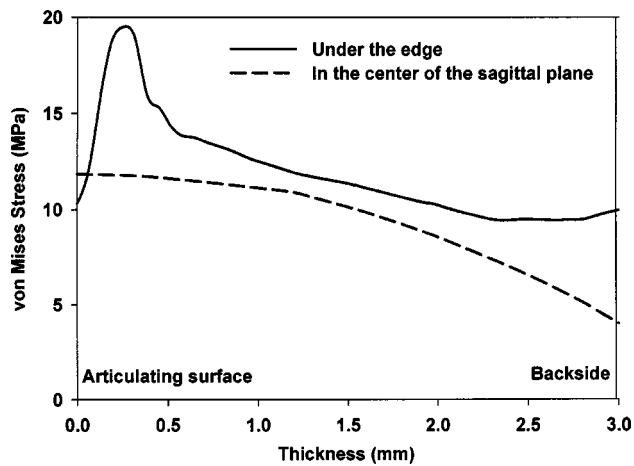

Fig. 3   von Mises stress on the Standard width polyethylene surface. (Neutral tibio-pedal angle.)

Fig. 7 von Mises stress through the thickness, at the edge and at the center of a sagittal plane cut (Standard width component)

Discussion

This study has provided a three-dimensional analysis of the polyethylene stresses and the influence of design variations in ankle replacement. The model includes a realistic representation of the material properties and structures and the tibio-fibular load distribution reflects validated physiologic conditions [23–26]. Therefore the results of this model can be expected to appropriately quantify the stresses in the polyethylene under the given assumptions.

The reduction in stress was generally less than that predicted in the hypothesis of the study. Assuming complete talar-polyethylene contact, the interface area increased by 36% at the neutral tibio-talar angle, but the stresses along the frontal plane at the midline decreased less than that. Furthermore, increasing the talar component width decreased the contact pressure at the edge (peak) more than the contact pressure at the center (Fig. 4). The contact pressures at the edge of the talar component dropped from 36 to 26 MPa (28%), while the value at the center fell from 24 to 20 MPa (17%). The edge and center von Mises stresses both declined by 17%, the edge value falling from 19.5 to 16.3 MPa and the center value from 11.4 to 9.3 MPa (Fig. 5). The von Mises stress is of short-term importance because it predicts yielding and plastic behavior and long-term importance because it may be related to delamination [27]. The contact pressure is of long-term importance because it is directly related to abrasive and adhesive wear.
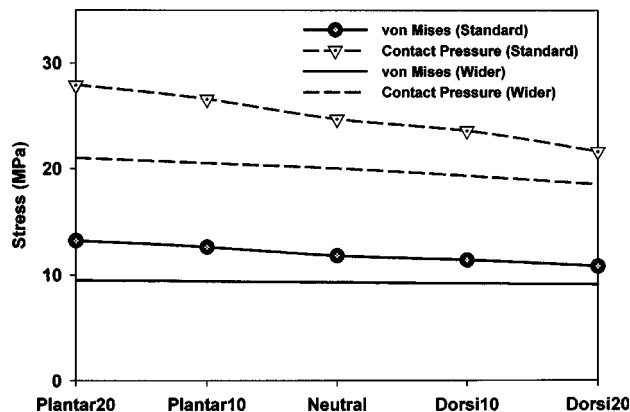

Fig. 8 von Mises stress and contact pressures in the polyethylene with respect to flexion angles at the midpoint of the talar components

The proportional limit of polyethylene [21] is approximately 11 MPa so that very little yielding can be expected for the wider design.

In considering the von Mises stresses through the thickness at the anterior-posterior midpoint, stresses approaching the yield stress occurred at the polyethylene surface and penetrated approximately one millimeter into the thickness (Fig. 7) for the narrower talar component. As can be expected in nonconformal Hertzian contact [28], the peak von Mises stress occurred beneath the surface under the edge of the talar component; the stress magnitudes approached or exceeded the yield stress all the way through the thickness. The von Mises stresses were less than those computed in knee replacements, 25 MPa [10].

The decreases in stress with dorsiflexion correlated with the increased anterior width of the talar component. However, the decrease in von Mises stress was smaller than the decrease in contact pressure. The wider talar component did not have this same decrease, of course, because the width was almost constant.

This study discounted several secondary effects such as edge loading by the talar component with inversion-eversion and torque around the tibial anatomic long axis. While inversion-eversion and axial rotation of the talus around the tibial long axis could theoretically occur, axial loading could force the components into conformal contact. This implant permits dorsi-plantar flexion and medial-lateral translation but could still transmit a torque. If a torque were applied, the most anteriorly and posteriorly located points of contact would have the largest moment arms to balance this torque. These are not the location of the peak stresses in the current study, so that the peak stresses may not change substantially under applied torque. Furthermore, unless a torque were applied by a pure couple or by forces with only anterior-posterior direction, lateral-medial translation could serve to reduce further the resulting stresses.

The computed contact stresses have implications for implant wear. Contact pressures for both implant widths in this study were less than the results of 55 MPa computed in knee replacements [10] and exceeded the 15 MPa computed for hip replacements [29], although it should be noted that the current study used a larger external load in order to simulate physiologic ankle loading. The higher edge pressures could lead to localized wear, which in turn could reduce the peak pressures through redistribution of the load. Although the volumetric wear rate will depend on the number of cycles per year, the localized wear of the polyethylene per cycle depends essentially on the pressure alone. Based on the known wear of polyethylene in the knee, this ankle implant should have better durability than current knee systems [30,31].

Some of the features omitted in this study will be addressed in future work. Inclusion of torque transmission through the joint could refine the results especially if variations with the gait cycle are also included. Loads due to accurately modeled muscle forces could also alter the stress distribution and, finally, modeling of the ligaments could redistribute the loads.

In conclusion, total ankle arthroplasty was authentically modeled with precise bone and implant geometry. Peak von Mises stresses were found to occur beneath the surface and analysis of two talar designs showed that the stresses in the polyethylene had many similarities to those in knee and hip implants. A larger bearing surface had expected benefits in reducing average and peak stresses and could potentially lead to a reduction in wear and cold flow, but the larger surface area did not proportionally reduce these stresses.

Acknowledgment

References

[1] Alvine, F. G., 1999, *Agility Total Ankle System, Surgical Technique*, DePuy a Johnson & Johnson, Warsaw, Indiana. pp. 10.
[2] Gould, G. S., Alvine, F. G., Mann, R. A., Sanders, R. W., and Walling, A. K.,

2000, "Total Ankle Replacement: A Surgical Discussion. Part I. Replacement Systems, Indications, and Contraindications," Am. J. Orthop., **29**(8), pp. 604–609.

[3] Gould, G. S., Alvine, F. G., Mann, R. A., Sanders, R. W., and Walling, A. K., 2000, "Total Ankle Replacement: A Surgical Discussion. Part II. The Clinical and Surgical Experience," Am. J. Orthop., **29**(9), pp. 675–682.

[4] Pyevich, M. T., Saltzman, C. L., Callaghan, J. J., and Alvine, F. G., 1998, "Total Ankle Arthroplasty: Unique Design, Two to Eleven Year Follow-up," J. Bone Jt. Surg., **80-A**(10), pp. 1410–1420.

[5] Saltzman, C. L., McIff, T. E., Buckwalter, J. A., and Brown, T. D., 2000, "Total Ankle Replacement Revisited," J. Orthop. Sports Phys. Ther., **30**(2), pp. 56–57.

[6] Harris, W. H., 1994, "Osteolysis and Particle Disease in Hip Replacement," Acta Orthop. Scand., **65**, pp. 113–123.

[7] Harris, W. H., 1995, "The Problem is Osteolysis," Clin. Orthop., **311**, pp. 46–53.

[8] Howie, D. W., 1990, "Tissue Response in Relation to Type of Wear Particles Around Failed Hip Arthroplasties," J. Arthroplasty, **5**, pp. 337–348.

[9] Wright, T. M., and Bartel, D. L., 1986, "The Problem of Surface Damage in Polyethylene Total Ankle Arthroplasty," Clin. Orthop. Relat. Res., **205**, pp. 67–74.

[10] Bartel, D. L., Rawlinson, J. J., Burstein, A. H., Ranawat, C. S., and Flynn, W. F., 1995, "Stresses in Polyethylene Components of Contemporary Total Knee Replacements," Clin. Orthop. Relat. Res., **317**, pp. 76–82.

[11] Maxian, T. A., Brown, T. D., Pedersen, D. R., and Callaghan, J. J., 1996, "A Sliding-Distance-Coulped Finite Element Formulation for Polyethylene Wear in Total Hip Arthroplasty," J. Biomech., **29**, pp. 687–692.

[12] Giannini, S., Leardini, A., and O'Connor, J. J., 2000, "Total Ankle Replacement: Review of the Designs and of Current Status," Foot Ankle Surgery, **6**, pp. 77–88.

[13] Calderale, P. M., Garro, A., Barbiero, R., and Fasolio, G., 1983, "Biomechanical Design of the Total Ankle Prosthesis," Eng. Med., **12**(2), pp. 69–80.

[14] Crowell, H. P., 1991, "Three Dimensional Finite Element Analysis of an Ankle Prosthesis," Innovative Technological Biological Medicine, **12**, pp. 2–12.

[15] Falsig, J., Hvid, I., and Jensen, N. C., 1986, "Finite Element Stress Analysis of Some Ankle Prosthesis," Clin. Biomech. (Los Angel. Calif.), **1**, pp. 71–76.

[16] Oonishi, H. e. a., 1984, *Cementless Alumina Ceramic Artificial Ankle Joint*, in *Biomaterials and Biomechanics*, edited by P. Ducheyne, Elsevier Science Publishers B. V., Amsterdam. pp. 85–90.

[17] Lewis, G., and Austin, G. E., 1994, "A Finite Element Analysis Study of Static Stresses in a Biomaterial Implant," Innovations and Technology in Biology and Medicine, **15**(5), pp. 634–644.

[18] McIff, T. I., 2001, "Contact and Internal Stress Distribution in Two Types of Contemporary 'Unconstrained' Total Ankle Designs," J. Biomech., **34**, pp. S23–S28.

[19] Kurtz, S. M., Edidin, A. A., and Bartel, D. L., 1997, "The Role of Backside Polishing, Cup Angle, and Polyethylene Thickness on the Contact Stresses in Metal-Backed Acetabular Components," J. Biomech., **30**(6), pp. 639–642.

[20] Alpas, A. T., Hu, H., and Zhang, J., 1993, "Plastic Deformation and Damage Accumulation Below the Worn Surfaces," Wear, **162−164**, pp. 188–195.

[21] DeHeer, D. C., and Hillberry, B. M., 1992, "*The Effect of Thickness and Nonlinear Material Behavior on Contact Stresses in Polyethylene Tibial Components*," 38th Annual Meeting of the ORS, **17**(2), pp. 327.

[22] Seireg, A., and Arkivar, R. J., 1975, "The Prediction of Muscular Load Sharing and Joint Forces in the Lower Extremities During Walking," J. Biomech., **8**, pp. 89–102.

[23] Goh, J. C. H., Lee, H., Ang, J., and Pho, W. H., 1992, "Biomechanical Study on the Load-Bearing Characteristics of the Fibula and the Effects of Fibular Resection," Clin. Orthop. Relat. Res., **279**, pp. 223–228.

[24] Skraba, J. S., and Greenwald, A. S., 1982, "Weight Bearing Role of the Human Fibula," Foot Ankle, **2**, pp. 345–346.

[25] Takebe, K., 1984, "Role of the Fibula in Weight-Bearing," Clin. Orthop. Relat. Res., **189**, pp. 289–292.

[26] Lambert, K. L., 1971, "The Weight-Bearing Function of the Fibula," J. Bone Jt. Surg., **53-A**(3), pp. 507–513.

[27] Estupinan, J. A., Bartel, D. L., and Wright, T. M., 1998, "Residual Stresses in Ultra-High Molecular Weight Polyethylene Loaded Cyclically by a Rigid Moving Indenter in Nonconforming Geometries," J. Biomed. Mater. Res., **16**(1), pp. 80–88.

[28] Rawlinson, J. J., and Bartel, D. L., 2002, "Flat Medial-Lateral Conformity in Total Knee Replacements Does Not Minimize Contact Stresses," J. Biomech., **35**, pp. 27–34.

[29] Bartel, D. L., Bicknell, V. L., and Wright, T. M., 1986, "The Effect of Conformity, Thickness, and Material on Stresses in Ultra-High Molecular Weight Components for Total Joint Replacement," J. Bone Jt. Surg., **68-A**(7), pp. 1041–1051.

[30] Pedersen, D. R., Brown, T. D., Hillis, S. L., and Callaghan, J. J., 1998, "Prediction of Long-Term Polyethylene Wear in Total Hip Arthroplasty Based on Early Wear Measurements Made Using Digital Image Analysis," J. Orthop. Res., **16**(5), pp. 557–563.

[31] Lewis, G., 1997, "Polyethylene Wear in Total Hip and Knee Arthroplasties," J. Biomed. Mater. Res., **38**(1), pp. 55–75.